Basin architecture and density structure beneath the Strait of Georgia, British Columbia[1]

C. Lowe, S.A. Dehler, and B.C. Zelt

Abstract: Georgia Basin is located within one of the most seismically active and populated areas on Canada's west coast. Over the last decade, geological investigations have resolved important details concerning the basin's shallow structure and composition. Yet, until recently, relatively little was known about deeper portions of the basin. In this study, new seismic velocity information is employed to develop a 3-dimensional density model of the basin. Comparison of the calculated gravity response of this model with the observed gravity field validates the velocity model at large scales. At smaller scales, several differences between model and observed gravity fields are recognized. Analysis of these differences and correlation with independent geoscience data provide new insights into the structure and composition of the basin-fill and underlying basement. Specifically, four regions with thick accumulations of unconsolidated Pleistocene and younger sediments, which were not resolved in the velocity model, are identified. Their delineation is particularly important for studies of seismic ground-motion amplification and offshore aggregate assessment. An inconsistency between the published geology and the seismic structure beneath Texada and Lasqueti Islands in the central Strait of Georgia is investigated; however, the available gravity data cannot preferentially validate either the geologic interpretation or the seismic model in this region. We interpret a northwest-trending and relatively linear gradient extending from Savory Island in the north to Boundary Bay in the south as the eastern margin of Wrangellia beneath the basin. Finally, we compare Georgia Basin with the Everett and Seattle basins in the southern Cascadia fore arc. This comparison indicates that while a single mechanism may be controlling present-day basin tectonics and deformation within the fore arc this was not the case for most of the Mesozoic and Tertiary time periods.

Résumé : Le bassin de Géorgie est situé dans l'une des régions les plus peuplées de la côte ouest du Canada et où l'activité sismique est très élevée. Au cours de la dernière décennie, les investigations géologiques ont permis de résoudre d'importants détails concernant la structure et la composition de ce bassin peu profond. Toutefois, jusqu'à tout dernièrement, peu était connu des portions plus profondes du bassin. Dans cette étude, de nouvelles informations de vitesse sismique servent à développer un modèle 3-D de la densité du bassin. Une comparaison entre la réponse de la gravité calculée à partir de ce modèle et le champ de gravité observé valide le modèle de vitesse à de grandes échelles. À de plus petites échelles, on reconnaît plusieurs différences entre les champs de gravité du modèle et ceux de terrain. L'analyse de ces différences et la corrélation avec des données géoscientifiques indépendantes fournit de nouveaux points de vue sur la structure et la composition du matériau de remplissage du bassin et celui du socle sous-jacent. Plus spécifiquement, on identifie quatre régions ayant des accumulations épaisses de sédiments non consolidés du Pléistocène et plus jeunes, qui n'ont pas été résolues dans le modèle de vitesse. Leur délimitation est particulièrement importante pour les études d'évaluation de l'amplification du mouvement du sol et des agrégats au large provoquée par les ondes sismiques. On examine la contradiction entre les données géologiques publiées et la structure sismique en dessous de Texada et des îles Lasqueti dans le centre du détroit de Géorgie; toutefois, les données gravimétriques disponibles ne peuvent valider de façon préférentielle l'interprétation géologique ou le modèle sismique dans cette région. Nous interprétons le gradient relativement linéaire, de direction nord-ouest, qui s'étend de l'île de Savory au nord et la baie Boundary au sud comme étant la bordure est de Wrangellia en dessous du bassin. Finalement, nous comparons le bassin de Géorgie avec les bassins d'Everett et de Seattle dans l'avant-arc du sud de Cascadia. Bien qu'un seul mécanisme puisse contrôler la tectonique et la déformation actuelles du bassin à l'intérieur de l'avant-arc, cette comparaison indique que cela n'était pas le cas pour la plus grande partie du Mésozoïque et du Tertiaire.

[Traduit par la Rédaction]

C. Lowe.[2] Geological Survey of Canada – Pacific, P.O. Box 6000, Sidney, BC V8L 4B2, Canada.
S.A. Dehler. Geological Survey of Canada – Atlantic, Bedford Institute of Oceanography, P.O. Box 1006, Dartmouth, NS B2Y 4A2, Canada.
B.C. Zelt. University of Hawaii, School of Ocean and Earth Science and Technology, 1680 East-west Road, Honolulu, HI 96822, U.S.A.

Introduction

Georgia Basin underlies the Strait of Georgia and adjacent coastal areas on Canada's west coast (Fig. 1). This populated area, located between the Juan de Fuca trench and the Cascade magmatic arc, is one of the most seismically active regions in the country. Recent felt events include a 1997, M 4.6 event, located 30 km west of Vancouver, that was felt throughout southwestern British Columbia and the Puget Sound region of Washington State (Cassidy et al. 2000). Protection of the area's population and infrastructures, mitigation of hazards, and management of potential resources contained within Georgia Basin require detailed knowledge of the crustal structure and basin composition. However, until recently such information was either unavailable or inadequately resolved to address these issues comprehensively.

In 1998, an extensive seismic program was conducted to investigate the crustal structure beneath the Strait of Georgia and Puget Lowland regions. The joint U.S.–Canada Seismic Hazard Investigation of Puget Sound (SHIPS) experiment (Fisher et al. 1999) provided a large volume of seismic reflection and refraction data that sampled the subsurface at high-resolution. Zelt et al. (2001) used first arrival travel-time data from numerous receivers within and bordering the Strait of Georgia to develop a 3-dimensional (3-D) velocity model of the upper crust using tomographic inversion. Their study provided the first detailed look at crustal velocity variations within the elongated Georgia Basin and sampled the crustal structure to depths of ~13 km with better resolution than any previous work (e.g., Zelt et al. 1996). This study extends their results by (*i*) deriving a forward gravity model from the velocity analysis and comparing the model-calculated gravity field with the observed gravity field over the Strait of Georgia to quantitatively assess the tomographic model, and (*ii*) examining the source of residual gravity anomalies from shallow and sub-basin depths to provide new information about the composition and structure of the basin-fill and underlying basement.

Tectonic setting

The geology and geological evolution of Georgia Basin are discussed in detail by Mustard (1994), Mustard and Rouse (1994), and England and Bustin (1998). Manuscripts by Monger (1990, 1991) and Monger and Journeay (1994) comprehensively describe the basement beneath the basin. Accordingly, only a brief summary is presented here.

The basin developed above three distinct basement units: Wrangellia to the west, the Coast Belt to the east, and the Cascade Mountains to the south and southeast (Fig. 1). Wrangellia comprises Paleozoic, Triassic, and Jurassic rocks. The Paleozoic section features an island-arc assemblage of variably metamorphosed, chiefly volcanic and sedimentary rocks. The Triassic interval is represented by thick basalt flows, pillow lavas, and tuffs with overlying limestones and argillaceous sediments. The Jurassic section consists of calc-alkaline volcanics and sediments and a coeval suite of granodiorites. Basement rocks in the Coast Belt adjacent to Georgia Basin consist of mainly Jurassic to mid-Cretaceous granite and granodiorite. Locally the granitic rocks carry roof pendants of stratified volcanic and sedimentary rocks.

In the Cascade Mountains, the basement consists of a variably metamorphosed assemblage of Mesozoic sedimentary strata and other diverse rock types. Along the south rim of Georgia Basin, in the northern San Juan Islands, there are several Upper Jurassic to possibly middle Cretaceous clastic formations. Beneath the basin, the locations and the nature of the boundaries among these three basement units are constrained poorly.

The first and most significant period of basin-wide subsidence occurred during the Late Cretaceous, resulting in the accumulation of several kilometres of dominantly marine siliciclastic deposits in the Nanaimo Group. Nanaimo Group strata unconformably overlie Wrangellia to the west, the Coast Belt to the east, and to the southeast they are in fault contact with the San Juan thrust system. The lower one third of the Nanaimo Group is a complex mix of nonmarine alluvial and mostly shallow-marine fine-grained sedimentary rocks, whereas the upper two-thirds is composed of mudstone and thin-bedded sandstone turbidites of dominantly deep-marine origin. This upper section includes conglomerates deposited in submarine fan systems.

During the latest Cretaceous to Early Paleocene there was a recession of marine waters, as well as uplift and erosion of basin units, especially in the southern part of Georgia Basin. Deformation was followed by a second phase of rapid subsidence in the Late Paleocene to Late Eocene and the accumulation of several kilometres of siliciclastic, mainly nonmarine sediments. Tertiary strata consist of nonmarine Paleogene sediments in the Huntington Formation (predominantly sandstones and shales) that are overlain by Neogene sedimentary rocks of the Boundary Bay Formation. Although the main Tertiary depocenters were in southeastern Georgia Basin, outliers of Paleogene sediments are preserved in northeastern Georgia Basin. Neogene sedimentation was restricted to the southeastern margin of the basin and is characterized by mixed marginal marine and fluvio-deltaic deposits. Today these Neogene sediments are preserved in the Fraser River delta subsurface.

Quaternary sediments are widely distributed over large areas of Georgia Basin, especially under the Strait of Georgia (Hamilton 1991; Mosher and Hamilton 1998) and adjacent coastal areas of eastern Vancouver Island (Clague 1977). These sediments are mainly glacial drift, but include fluvial, estuarine, and marine sediments. In southeastern Georgia Basin, up to 1 km of fluvial, flood plain, deltaic, and associated estuarine and marine sediments of the Fraser River system overlie Pleistocene deposits (Mathews and Shepard 1962; Clague et al. 1983; Hunter et al. 1998).

Georgia Basin was deformed during a major contractional event in the Tertiary. Deformation, which was coeval with accretion of the Pacific Rim and Crescent terranes to Wrangellia (Fig. 1), resulted in the development of (*i*) southwest-directed thrusts and up to 30% (10–30 km) shortening of Nanaimo Group strata in southwestern Georgia Basin and (*ii*) northwest-plunging and -trending folds in the Chukanut Formation in southeastern Georgia Basin (Johnson 1984). Recently, Journeay and Morrison (1999) documented a younger, Late Oligocene to Early Miocene, deformation event that involved much of the southern part of Georgia Basin and resulted in a sinuous belt of northwest-trending buckle folds, northeast-vergent thrust faults, and minor extensional faulting. Today, the Mesozoic

Fig. 1. Regional setting of the study area (after Monger 1990; England and Bustin 1998; Zelt et al. 2001). Solid grey shading denotes exposures of sedimentary strata composing Georgia Basin. The large rectangular outline denotes the extent of the Zelt et al. (2001) tomographically derived velocity model and the density model discussed herein. The black star in central Strait of Georgia denotes the epicentre of the 1997 M 4.6 earthquake. Collectively, islands to the southeast of Nanaimo in Canadian waters, including Galiano Islands, are known as Gulf Islands. BB, Boundary Bay; BI, Bowen Island; CR, Crescent Terrane; FR, Fraser River; GI, Galiano Island; LI, Lasqueti Island; PR, Pacific Rim Terrane; PRB, Point Roberts; PS, Puget Sound; SEP, Sechelt Peninsula; SJF, San Juan Thrust System; SJI, San Juan Islands; SOG, Strait of Georgia; SP, Saanich Peninsula; TI, Texada Island. Inset map shows the plate tectonic setting and the main physiographic subdivisions of the Canadian Cordillera: I, Foreland Belt; II, Omineca Belt; III, Intermontane Belt; IV, Coast Belt; V, Insular Belt.
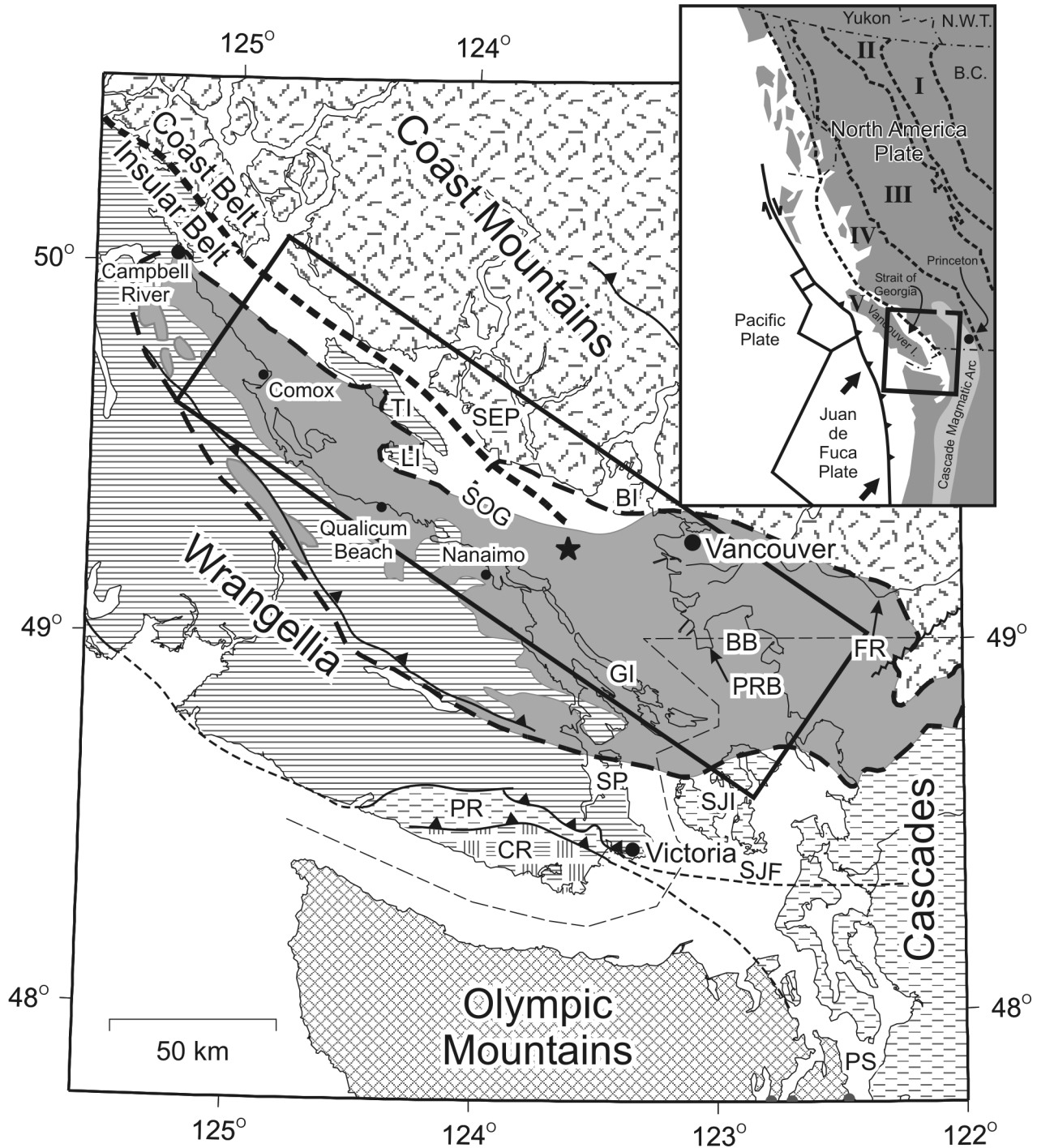
Fig. 2. Observed gravity (free-air offshore, Bouguer onshore) data in southwestern British Columbia. The study area is outlined by the large black rectangle. Very small dots denote the locations of the gravity stations. BI, Bowen Island; LI, Lasqueti Island; TI, Texada Island; SJI, San Juan Island.
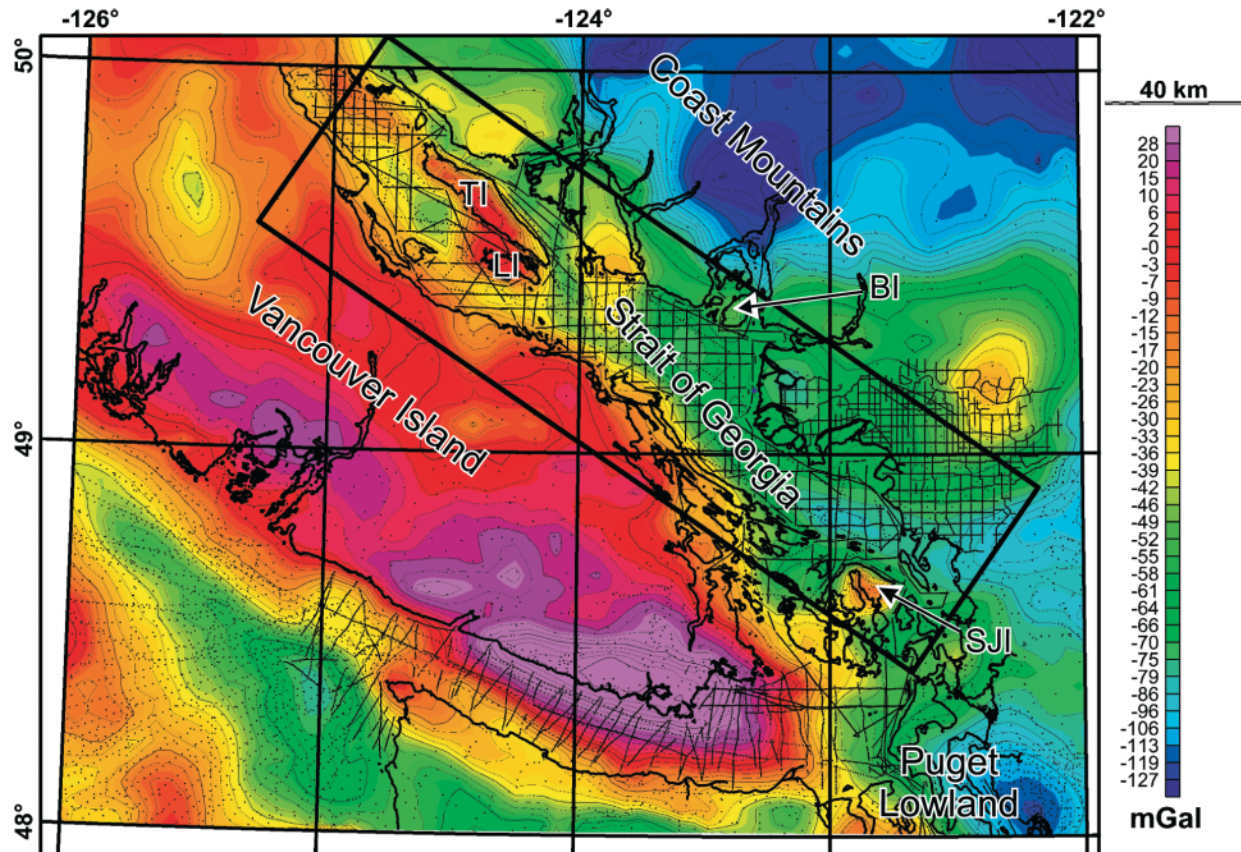
and Cenozoic sedimentary rocks that compose Georgia Basin are distributed over an area of some 25 000 km² (Fig. 1). However, throughout much of its depositional history the basin is thought to have covered a much larger area to the west, east, and northwest.

Gravity observations over the Strait of Georgia

A 2-km grid of the combined free-air gravity (offshore) and Bouguer anomaly (onshore) was generated for southwestern British Columbia from data supplied by Geomatics Canada, Department of Natural Resources, Ottawa, Ontario (Fig. 2). Offshore data consisted mainly of shipborne measurements along lines spaced generally 3–9 km apart and some sea-bottom measurements. Onshore, a high-resolution survey of the Fraser River delta and adjacent parts of the lower mainland provided measurements every 400 m on north- and east-trending lines spaced ~2–4 km apart. Elsewhere, measurements are typically 10 km apart. Onshore measurements are terrain corrected and considered accurate to ±1 mGal, whereas offshore measurements are considered accurate to ±2 mGal. More than 15 000 gravity measurements constrain the gravity field within the area of this study (outlined by black rectangle in Fig. 2).

In general, the gravity field in southwestern British Columbia is dominated by a regional northeasterly decrease in gravity values toward the Coast Mountains and a northwest-trending high on Vancouver Island. Low gravity values are observed in the offshore west of Vancouver Island, as well as over the Strait of Georgia, lower mainland and northern Puget Lowland, where thick accumulations of low-density unconsolidated sediments and sedimentary rocks occur. A broad, positive anomaly is coincident with higher density rocks of the Wrangellia Terrane on Vancouver Island, and a prominent positive anomaly over the southern tip of the island correlates with the surface outcrop of the Crescent Terrane (see Fig. 1). These regional gravity variations are interpreted and discussed by several authors, including Riddihough (1979), Dehler and Clowes (1992), and Clowes et al. (1997).

Within the study area, gravity values average about 40 mGal higher in the northern Strait of Georgia compared with the southern part of the strait. Distinct minima are observed to the north of the San Juan Islands, to the southwest of Bowen Island, and over coastal portions of the Fraser River delta. Isolated positive gravity anomalies are observed over Texada and Lasqueti islands in the northern Strait of Georgia. To the south of Nanaimo a prominent horizontal gravity gradient of 1.4 mGal/km is observed along the eastern edge of the Gulf Islands. The regional northeasterly decrease in gravity values, discussed earlier in the text, is also visible across the study area.

Model development

The crustal velocity model of Zelt et al. (2001) was used to construct the initial density model. Assuming that the

basement interface was defined by the 6.0 km/s isovelocity surface, their model indicated that Georgia Basin is highly asymmetric, with sediment thickness increasing from 2–4 km beneath the northern Strait of Georgia to ~8–9 km beneath the southeastern portion of the strait. Velocities range from 3 km/s at the surface to 6 km/s at the basement interface. Basin velocities ranging from 4.5–6.0 km/s were attributed to the Late Cretaceous Nanaimo Group, whereas velocities < 4.5 km/s were interpreted as Tertiary and younger deposits. In contrast to the relatively smoothly varying velocity structure of the basin, basement velocities in their model showed significant lateral variations.

Isovelocity contours between 3.0 and 6.0 km/s were extracted from the velocity model at 0.5 km/s intervals to define a series of six sedimentary horizons and the basement interface. In general, the velocity model was not well constrained near surface due to few short-offset ray paths, and average lateral resolution at shallow depths was estimated as 10 km by Zelt et al. (2001). Independent data sets were thus used to define the sea floor and two shallow sedimentary layers. The base of the uppermost (water) layer was defined using gridded 2 arc-minute bathymetry data, derived from satellite altimetry data, provided by Scripps Institute of Oceanography, San Diego, California. Layer 2, representing Holocene fluvio-deltaic deposits of the Fraser Lowlands, was defined using maps presented in Hunter et al. (1998). These authors based their interpretation of deltaic sediment thickness in onshore and offshore areas on borehole, seismic reflection and refraction, and other remotely sensed data. Layer 3, which extends from the base of layer 2 to the top of the 3.0 km/s isovelocity horizon, is assumed to represent Pleistocene glaciomarine deposits.

All layer boundaries, including those extracted from the original 0.8 km-gridded velocity model, were gridded at 2 km intervals (identical to the gravity grid) using a weighted minimum curvature algorithm (Smith and Wessel 1990). The bottom surfaces of the 9 layers in this model are shown in Fig. 3. Layer thicknesses were smoothly extrapolated and (or) tapered to zero outside areas of data coverage prior to gridding to extend coverage across the entire model space. However, it should be noted that in some areas, e.g., south and east of Boundary Bay, layer depths are poorly constrained. These regions are omitted in the final interpretation.

A density of 1030 kg/m^3 was assigned to the water layer. Layers 2 (Holocene sediments) and 3 (Pleistocene sediments) were assigned densities of 1900 and 2100 kg/m^3, respectively, consistent with measured values reported in Dallimore et al. (1995) and information provided by J. Hunter (unpublished data). For the initial model, densities of all underlying sedimentary layers were computed from their seismic velocities using the empirically derived logarithmic relationship of Gardner et al. (1974)

$$\rho = 1740 \ v^{0.25}$$

where ρ and v represent density (kg/m^3) and seismic velocity (km/s), respectively, (Table 1). Model densities were assigned relative to basement, for which a density value of 2730 kg/m^3 was chosen, the mean of 357 samples of Wrangellian lithologies (Table 2). The gravitational attraction of the mass of each layer was calculated in the Fourier domain using the

Table 1. Model densities.

Layer #	Density (kg/m^3) (a)	(b)	Interpretation
1	1030	1030	water
2	1900	1900	Holocene, fluvio-deltaic deposits of the Fraser Lowlands
3	2100	2100	unconsolidated Pleistocene glaciomarine deposits
4	2290	2510	Boundary Bay, Huntington–Chukanut Formations
5	2380	2510	
6	2461	2510	
7	2534	2630	Nanaimo Group
8	2602	2630	
9	2665	2630	

Note: (a) Starting model: densities of layers 4–9 were computed from the seismic velocities using the empirical relationship of Gardner et al. (1974); (b) Refined model: densities of layers 4–6 and 7–9 were assumed to represent sedimentary rocks of the Huntington Formation and Nanaimo Group, respectively, and assigned densities consistent with measured values (see Table 2 and text). In both (a) and (b) the densities of layers 2 and 3 are consistent with values published in Dallimore et al. (1995) and J. Hunter (unpublished data).

method of Parker (1972), and the results summed to give the total model response.

Although the gravity response of this starting model reproduced major features in observed gravity data, there were several noteworthy differences between the two fields and the process was subsequently repeated using basin-fill densities determined for surface outcrop samples. The average density of the Tertiary Huntington Formation is 2510 kg/m^3, and the Late Cretaceous Nanaimo Group is 2630 kg/m^3 (Table 2). Density determinations were conducted on samples that spanned the Upper to Lower Huntington Formation, and Upper to Middle Nanaimo Group, however no systematic increase in density with age was observed within either unit. Consequently, in the refined input model a density of 2510 kg/m^3 was assigned to layers 4–6, representing units with velocities < 4.5 km/s in the Zelt et al. (2001) model, and a value of 2630 kg/m^3 to layers 7–9, representing the Nanaimo Group with velocities of 4.5 to 6.0 km/s. Densities for the shallower units and water layer remained the same as the starting model (Table 1). The gravity response of this refined density model (Fig. 4b) provided a better match to the observed data than that of the starting model: the relative amplitudes of several small-scale anomalies and the locations and extent of distinct gravity minima in the southern Strait of Georgia and to the west and north of Lasqueti Island were better correlated. This finding, together with a comparison of input densities for the starting and refined models (Table 1) suggests that the Gardner et al. (1974) velocity-density relation underestimates basin-fill densities for Georgia Basin. The finding contrasts with results obtained for other sedimentary basins in the Cascadia fore arc where Gardner et al.'s relation provides a good approximation for basin-fill densities (e.g., Brocher et al. 2001).

Major features and trends in the observed gravity field are well represented in the model-generated field (compare

Fig. 3. Depth to the base of each of the 9 layers in the input gravity model. The upper surface of the model is mean sea level. (*a*) base of water layer; (*b*) base of Holocene sediments; depth to isovelocity horizon (*c*) 3.0 km/s; (*d*) 3.5 km/s; (*e*) 4.0 km/s; (*f*) 4.5 km/s; (*g*) 5.0 km/s; (*h*) 5.5 km/s; and (*i*) 6.0 km/s. See text for data sources and details.
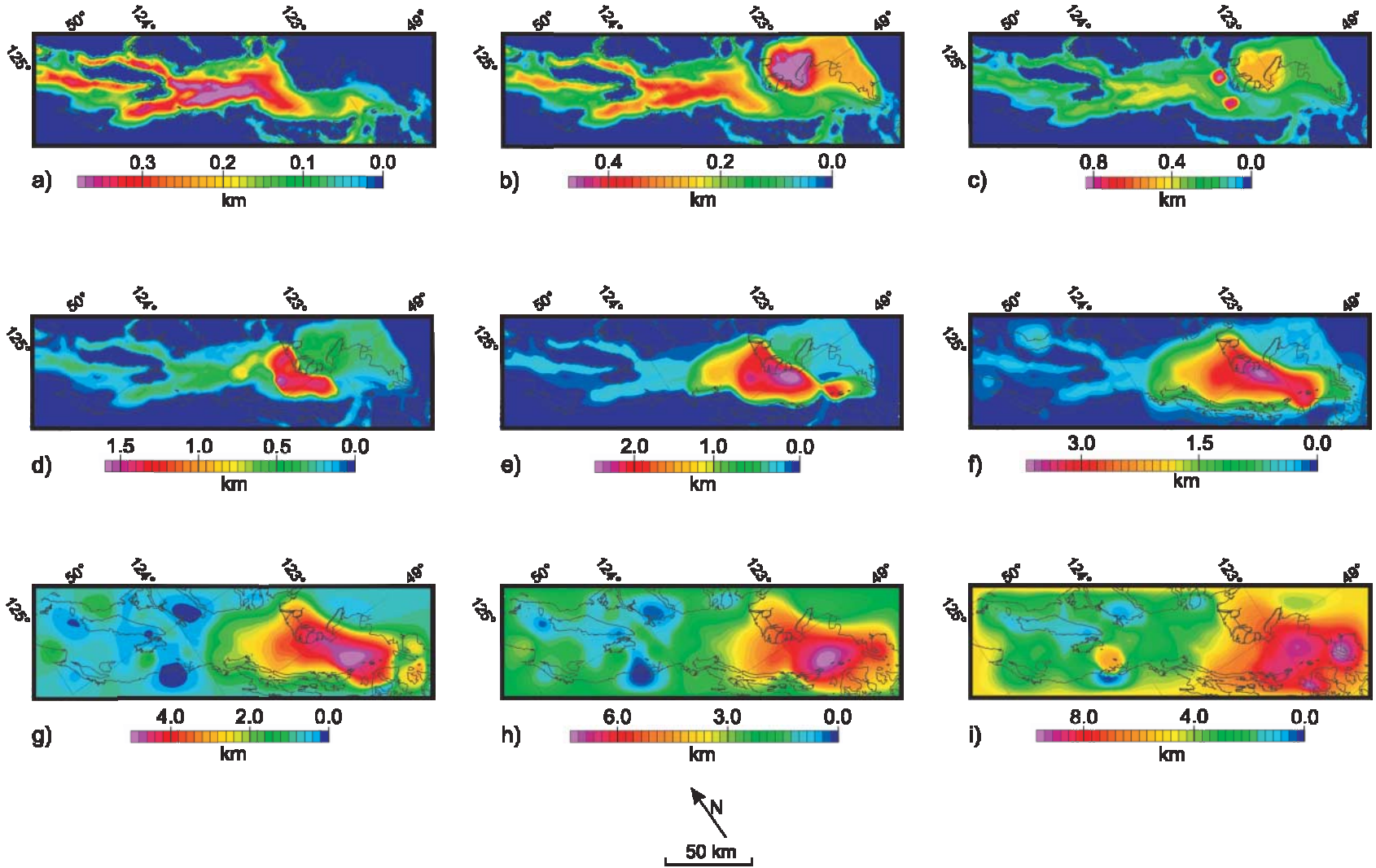
Table 2. Measured density and magnetic susceptibility values of geological units comprising Georgia Basin, Wrangellia, and the Southern Coast Belt.

Geological Unit	Density (kg/m^3)			Magnetic susceptibility (x 10^{-3} SI)		
	Mean	Range	#	Mean	Range	#
Georgia Basin						
Huntington Fm.	2510 ± 40	2430–2550	7	2.33 ± 6.53	0.08–32.2	24
Nanaimo Gp.	2630 ± 90	2350–2960	144	1.69 ± 2.31	–0.02–14.20	144
Gabriola Fm.	2630 ± 70	2350–2700	62	1.50 ± 1.54	0.22–3.97	62
Spray Fm.	2590 ± 140	2400–2700	14	0.28 ± 0.08	0.22–0.52	14
De Courcy Fm.	2630 ± 20	2580–2660	22	2.13 ± 1.31	0.59–3.19	22
Cedar Fm.	2590 ± 30	2540–2670	33	0.73 ± 1.02	0.24–3.10	33
Wrangellia						
Bonanza Gp.	2650 ± 180	1980–2790	38	18.40 ± 20.06	–0.06–57.60	40
Vancouver Gp.	2840 ± 140	2380–3130	124	9.53 ± 16.75	–0.09–107	146
Parson Bay Fm.	2620 ± 140	2380–2740	5	-0.03 ± 0.03	–0.06–0.01	5
Quatsino Fm.	2720 ± 60	2670–2950	21	2.49 ± 2.14	–0.09–5.21	39
Karmutsen Fm.	2880 ± 130	2500–3130	98	12.69 ± 19.16	0.14–107	102
Sicker Gp.	2790 ± 110	2380–3090	115	3.05 ± 9.59	–0.12–85.20	115
Mt. Mark Fm.	2740 ± 80	2640–2840	10	0.07 ± 0.24	–0.12–0.64	8
Cameron River Fm.	2750 ± 110	2540–2970	24	1.90 ± 4.66	–0.01–20.90	25
McLaughlin Fm.	2770 ± 120	2380–3090	108	2.76 ± 7.90	–0.05–53.70	109
Nitnat Fm.	2840 ± 90	2590–3020	63	4.67 ± 13.97	–0.02–85.20	63
Duck Lake Fm.	2780 ± 80	2680–2860	5	1.18 ± 1.59	0.24–3.98	5
Island Intrusions	2770 ± 110	2570–3070	55	16.90 ± 15.99	–0.10–76.20	56
Southern Coast Belt						
Coast Intrusions	2750 ± 87	2130–3150	921	14.5 ± 11.7	0–114	935
Gabbro	2990 ± 63	2900–3150	33	40.2 ± 31.3	1.12–114	33
Diorite	2810 ± 55	2630–2940	136	17.1 ± 11.0	0.1–51.6	140
Quartz diorite	2740 ± 70	2130–2910	514	14.9 ± 8.7	0.01–57.6	522
Quartz monzodiorite	2710 ± 45	2630–2810	78	10.7 ± 6.8	0.06–38.7	80
Granodiorite	2680 ± 40	2630–2840	117	8.25 ± 5.61	0–32.2	117
Quartz monzonite	2650 ± 25	2630–2730	18	7.29 ± 4.7	0.14–20.3	18
Granite	2640 ± 25	2580–2700	27	5.83 ± 4.97	0–18.8	27
Gambier Group	2790 ± 80	2540–3040	99	8.97 ± 14.7	0–82	117
Mesozoic metasediments	2800 ± 10	2630–2960	28	7.70 ± 9.68	0.05–32.1	29
Bowen Island Group	2830 ± 13	2600–3090	30	6.14 ± 12.4	0.02–50.3	35

Note: Density values for the Southern Coast Belt are courtesy of J.A. Roddick. #, number of samples; Fm., Formation; Gp., Group.

Figs. 4*a*, 4*b*), including higher average gravity values over the northern Strait of Georgia compared with the southern strait, isolated positive anomalies over Lasqueti and Texada islands, and a strong gravity gradient along the outer Gulf Islands. This general consistency between the two gravity fields validates the tomographically derived structural model of the basin at large scales. However, at smaller scales, there are a number of significant mismatches between the observed and computed fields. Some of these discrepancies may be attributed to the presence of lateral variations in the density of crustal rocks at depths below the model boundary, or to intra-basin mass variations which were not resolved in the seismic model. The wavelength of the mis-match provides some insight into the nature of the discrepancy as does correlation with independent geoscience observations. For example, one of the most notable differences between the two gravity fields is a long-wavelength, northeasterly decrease in gravity values that is clearly present in the observed field (Fig. 4*a*), but only weakly observed in the model-generated field (Fig. 4*b*). This gradient can be attributed, in large part, to the 5 km increase in crustal thickness from eastern Vancouver Island to the Coast Mountains (the increase is clearly imaged in seismic refraction data, e.g., Zelt et al. 1996). A first-order trend surface, approximating the gravity effect of increasing crustal thickness and other lower crustal variations, was removed from the observed gravity data (Fig. 4*c*) to better facilitate an analysis of additional mis-matches.

Figure 5*a* shows the difference between the observed (Fig. 4*c*) and model-calculated (Fig. 4*b*) gravity fields. As previously noted, the edges of the seismic model and the area to the east and south of Boundary Bay were poorly constrained in the velocity model, hence we do not show anomalies in these areas. Furthermore, the 2-km grid interval employed for all model input data precluded accurate definition of short-wavelength variations in bathymetry, unconsolidated sediment, and velocity layer thicknesses accounting for some of the observed short-wavelength differences. In recognition of this and other model limitations, we restrict our subsequent analysis of observed differences to those anomalies with spatial dimensions considerably greater than our grid interval and amplitudes ≥10 mGal. Several "local" and "regional" gravity difference anomalies meeting these criteria

Fig. 4. Gravity data in study area: (*a*) observed gravity; (*b*) model gravity computed using the layer densities listed in Table 1(b); (*c*) observed gravity with first-order trend removed. See text for additional details.
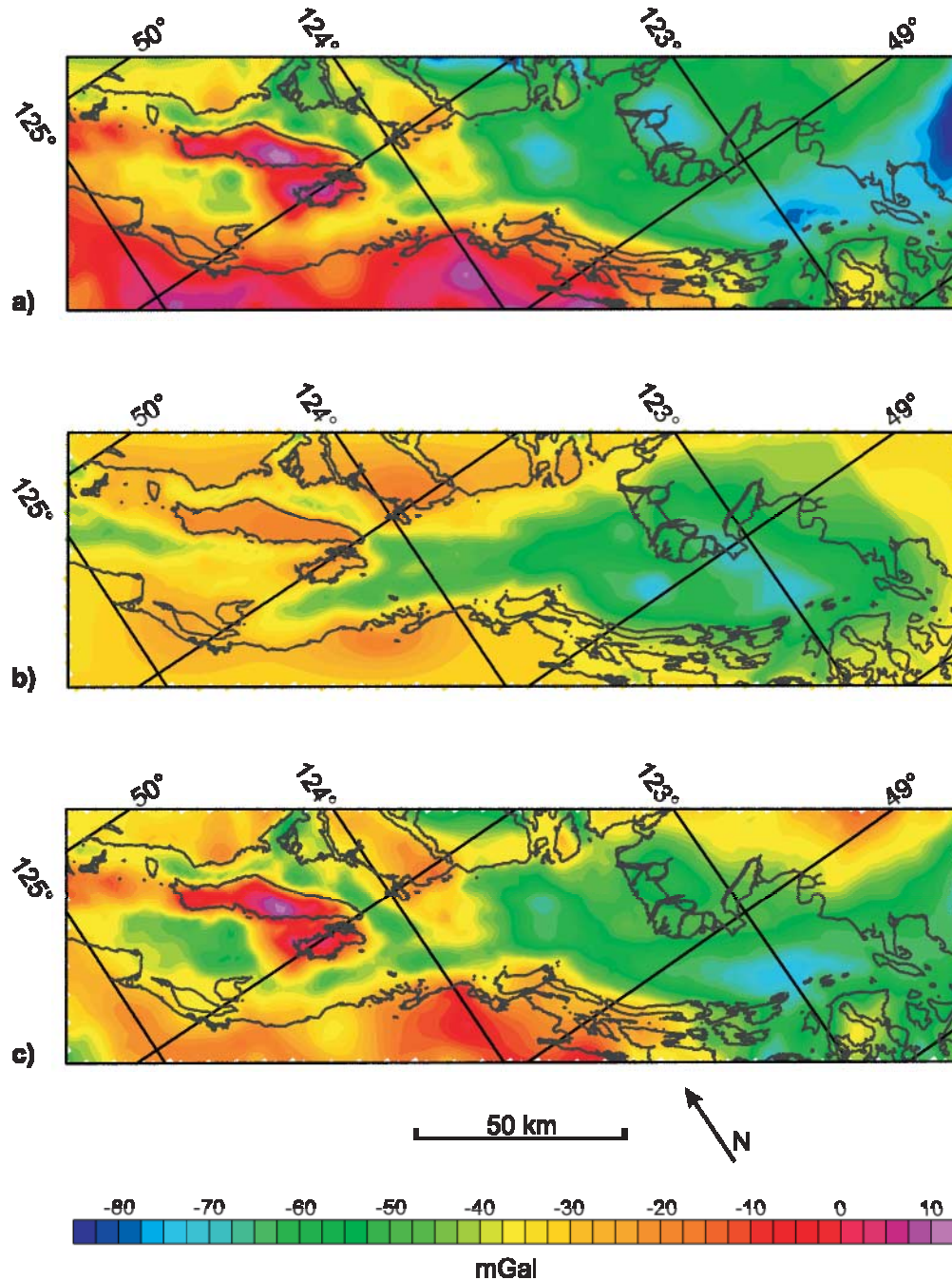
(see numbers and northwest-trending dashed line in Fig. 5*a*) were examined to determine the nature of their source and ascertain if they reflect lateral variations in the density of crustal rocks at depths below the model boundary or the presence of intra-basin density distributions, which were not resolved in the seismic model.

Interpretation of residual anomalies

(1) Intra-basin mass anomalies

Anomaly 1 (Fig. 5*a*) occurs in the Strait of Georgia between northern Texada and Hornby islands, where the

seismically estimated depth-to-basement is ~4 km. Here, in a sub-oval region, ~14 km × 12 km, gravity differences are –16 to –22 mGal (i.e., model calculated gravity values are 16 to 22 mGal higher than observed values), suggesting that the model either overestimates mass in this portion of the basin, or there is a mass deficiency in the underlying basement. The wavelength of the anomaly would imply a maximum source depth of ~6 km, although we note that gravity differences are also low for some kilometres surrounding this anomaly, allowing for a somewhat greater source depth.

There is no evidence of a spatially corresponding velocity anomaly in the basement beneath this region (coverage and

Fig. 5. (*a*) Residual gravity data obtained by subtracting the data displayed in Fig. 4*b* from that displayed in Fig. 4*c*. No data are shown for regions that were constrained poorly in the seismic model. The short-dashed line extending from Boundary Bay in the south to Savory Island in the north denotes the approximate Wrangellia (Insular Superterrane) – Coast Belt transition discussed in text. Long-dashed, N-trending line in the southern Strait of Georgia locates the 2-D seismic profile interpreted by Zelt et al. (2001), and the white star marks the location of a sub-basin lateral velocity discontinuity delineated by those authors. See text for discussion of anomalies 1 to 5. L100, L200, and L300 denote the locations of gravity models shown in Fig. 6. (*b*) Residual magnetic anomaly data for the model area showing the extent of anomaly 1 and the approximate eastern limit of Wrangellia from (*a*).
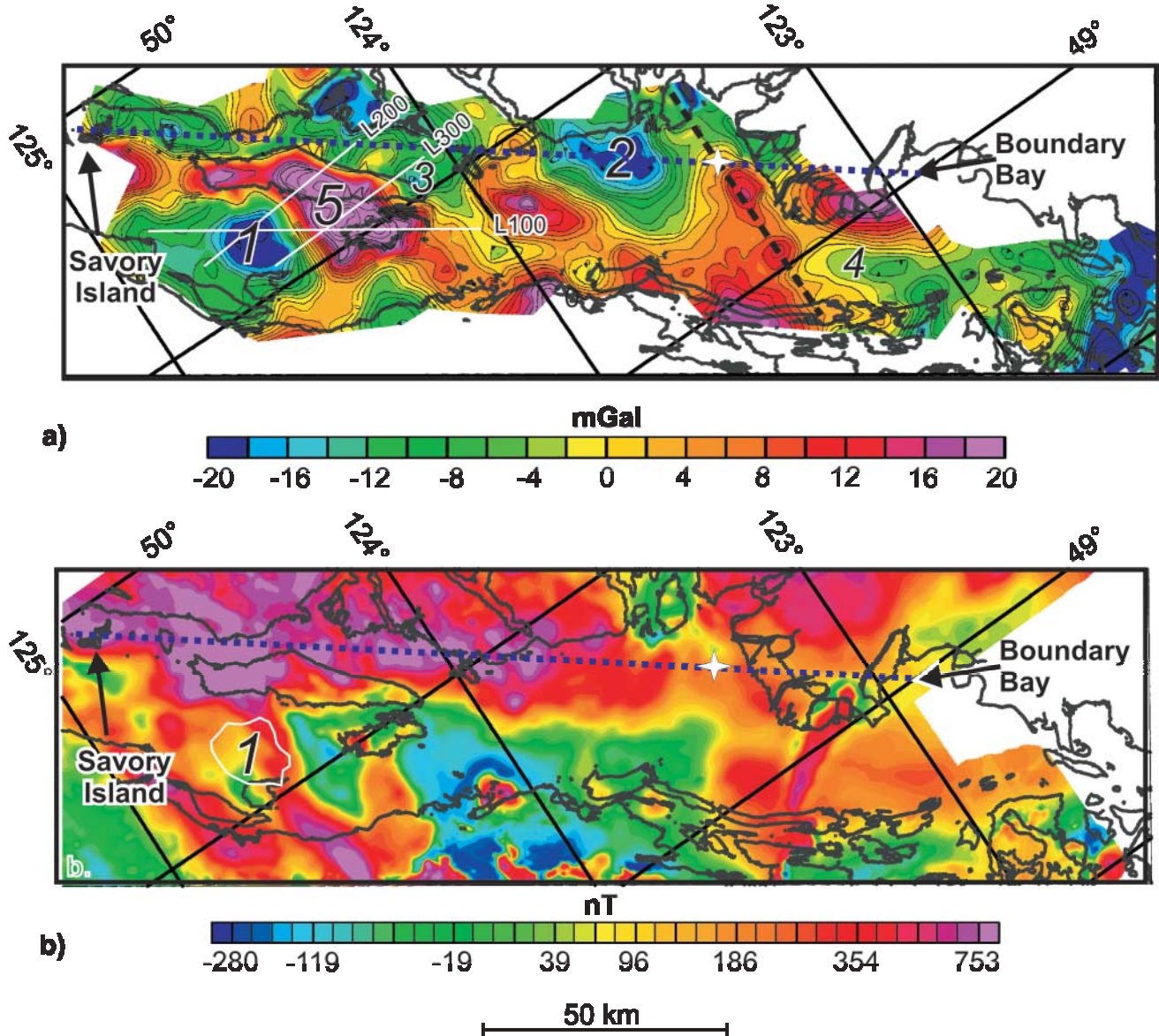
resolution of basement velocities are good to depths of 7 km). Nor is there any evidence of a coincident magnetic anomaly that could provide insight into the observed gravity discrepancy. Rather, examination of the available magnetic data (Fig. 5*b*) indicates that the basement is heterogeneous in this region. The southern half of the anomalous region corresponds with a north-trending zone, ~9 km wide, of elevated magnetic anomalies that can be traced from western Texada Island directly to exposures of highly magnetic (Table 2) Island Intrusions to the west of Georgia Basin on Vancouver Island. The width of the magnetic anomaly implies that the intrusion(s) must lie very close to the top of the basement.

The northern half of the anomalous region is characterized by lower amplitude magnetic anomalies, more typical of those observed over (lower susceptibility) Wrangellian units, such as the Vancouver or Sicker Group (Table 2).

Where well-constrained (at depths > 1 km), basin-fill velocities in the anomalous region are everywhere > 4.5 km/s and consequently, were entirely attributed to the Nanaimo Group. The measured variation in density of the Nanaimo Group is approximately ±3% (Table 2). A 3% density reduction over a 4 km depth interval would generate a –13 mGal anomaly, substantially less than the observed difference. However, if the uppermost 800 m of basin-fill in this region,

which was poorly constrained in the velocity model, were composed of Pleistocene or younger deposits (mean density ≤2100 kg/m^3; Dallimore et al. 1995), this would result in a –18 to –24.5 mGal or larger anomaly, more than sufficient to account for the observed discrepancy within data uncertainties. Preliminary interpretations of recently acquired shallow geophysical data and sediment cores from this area would support this latter scenario (Barrie and Conway 2000; Barrie, unpublished data). These new data indicate that a minimum of 300 m of unconsolidated Quaternary sediments (including more than 60 m of Holocene deposits) underlie much of the sea floor in this region. However, as neither the cores nor the seismic data sampled the underlying consolidated basin-fill rocks a substantially greater thickness of low-density Quaternary sediments is possible. Thus, the available evidence suggests that the source of the gravity discrepancy in this region is most likely attributable to the presence of a thick section of low-density Quaternary sediments that were not resolved in the velocity model and hence not included in the input gravity model. The finding is important for hazard studies as the anomalous region borders an important cable route for transporting power to Vancouver Island. Understanding and mitigating the risks posed by the amplification of seismic energy and (or) liquifaction in this seismically active region requires accurate knowledge of the distribution, composition, and thickness of all surficial sediments.

Anomaly 2 is located in central Strait of Georgia to the west of Bowen Island (Fig. 5a). This elongate difference anomaly is comparable in size to anomaly 1 (16 km × 9 km), but of slightly lower amplitude (–12 to –19 mGal). In this case, the velocity model is well constrained at depths between 2 and 6 km. At shallower depths, insufficient sampling by ray paths results in very poor velocity control, whereas at depths greater than 6 km, the eastern portion of the anomalous region is not well constrained. The seismically determined depth-to-basement ranges from 3 km in the north and east of the anomalous area to 4 km in the south and west. Where constrained, basin velocities are everywhere >3 km/s in this area and consequently, in the input gravity model, basin-fill was attributed to either the Tertiary Huntington Formation (where velocities are 3–4.5 km/s) or to the Late Cretaceous Nanaimo Group (where velocities exceed 4.5 km/s).

However, interpretations of high-resolution shallow geophysical and sediment core data in central and southern Strait of Georgia indicate that unconsolidated Quaternary and Recent sediments are pervasive beneath the sea floor in this region (Hamilton 1991; Mosher and Hamilton 1998). Indeed, these interpretations indicate that the thickest (> 500 m) section of pre Late Wisconsinan sediments occurs in the area of anomaly 2, and it is overlain by up to 100 m of younger glacial and Holocene sediments. The presence of these low-density sediments, which were not included in the input gravity model could account for more than 90% of the observed gravity difference. There is little evidence of a corresponding mass deficiency in the underlying basement that could contribute to the observed discrepancy: basement velocities in the anomalous region cannot be distinguished from those of adjacent areas to at least depths of 10 km. At greater depths, between 11 and 12 km, velocities over the

western portion of the anomaly are 0.2 km/s higher than other parts of the anomalous area (Zelt et al. 2001). However, a mass excess at these depths is unlikely to have a significant contribution to the observed difference anomaly, as the latter has a maximum wavelength of ~16 km.

Hamilton (1991) and Mosher and Hamilton (1998) identified two other areas of thick Quaternary sediments within their study area that were not included in our input model. Their shallow seismic data imaged ~350 m of unconsolidated sediments to the east of southern Texada Island (anomaly 3, Fig. 5a) and ~500 m of unconsolidated sediments at the extreme south of their survey area, between Galiano Island and Point Roberts Peninsula (anomaly 4, Fig. 5a). Inclusion of these sediments would reduce the model calculated gravity values by ~8–11 mGal and ~9–13 mGal, respectively, (as all basin-fill in the former area was attributed to the Nanaimo Group, whereas in the latter area the upper 2.5 km was attributed to the lower density Tertiary rocks) and would thereby eliminate most of the difference between observed and model-calculated gravity fields in these regions. The discrepancy observed between Galiano Island and Point Roberts persists south of the area investigated by Hamilton (1991) and Mosher and Hamilton (1998) suggesting that a trough of unconsolidated Pleistocene and Holocene sediments may extend southwards into southernmost Strait of Georgia. To date, there has been relatively little investigation of the aggregate potential of unconsolidated sediments in British Columbia's offshore areas. However, as local aggregate sources around the main population centers are increasingly depleted (Hora 1998), the need to identify new sources proximal to these centers becomes increasingly important. Anomalies 1 to 4 represent prospective targets within offshore Georgia Basin. Furthermore, our findings suggest that high-resolution gravity data could be an effective tool for aggregate mapping in offshore areas.

(2) Sub-basin mass anomalies

One of the largest difference anomalies occurs in an irregular-shaped region in the vicinity of Lasqueti and Texada islands (anomaly 5, Fig. 5a). Here, model-calculated gravity values are almost 29 mGal lower than observed values, implying that either the model underestimates mass within this portion of the basin, or alternatively, that there is an excess crustal mass in the basement beneath the islands. As noted earlier in the text, Zelt et al. (2001) did delineate velocity variations within the basement, including a distinct high-velocity (>6.5 km/s) body at shallow depths beneath these islands. 2.5-D gravity models were developed for three profiles that cross the anomaly (see locations on Fig. 5a) to ascertain if a corresponding high-density mass could account for the observed difference. The models (Option A, Fig. 6) used sedimentary layers constrained in depth by the velocity model and employed densities identical to those used in the refined gravity model (Table 1, column b). Results show that, with inclusion of a high-density (2900 kg/m^3) body corresponding spatially with the high-velocity body delineated by Zelt et al. (2001) (and low density layers at shallow depths (<1 km) corresponding to anomalies 1 and 3 discussed earlier in the text), the observed difference anomaly is matched well along L100 and L300. The peak amplitude of the observed residual on profile L200 is underestimated by ~7 mGal, but all other anomaly characteristics are matched well. As such,

Fig. 6. 2.5-D gravity models along profiles L100 (left), L200 (centre), and L300 (right). In each case the upper plot compares observed difference data with model-calculated gravity data for the three density models shown beneath (Options A, B, and C). See text for details. Profile locations are shown in Fig. 5. L.I., Lasqueti Island; T.I., Texada Island.
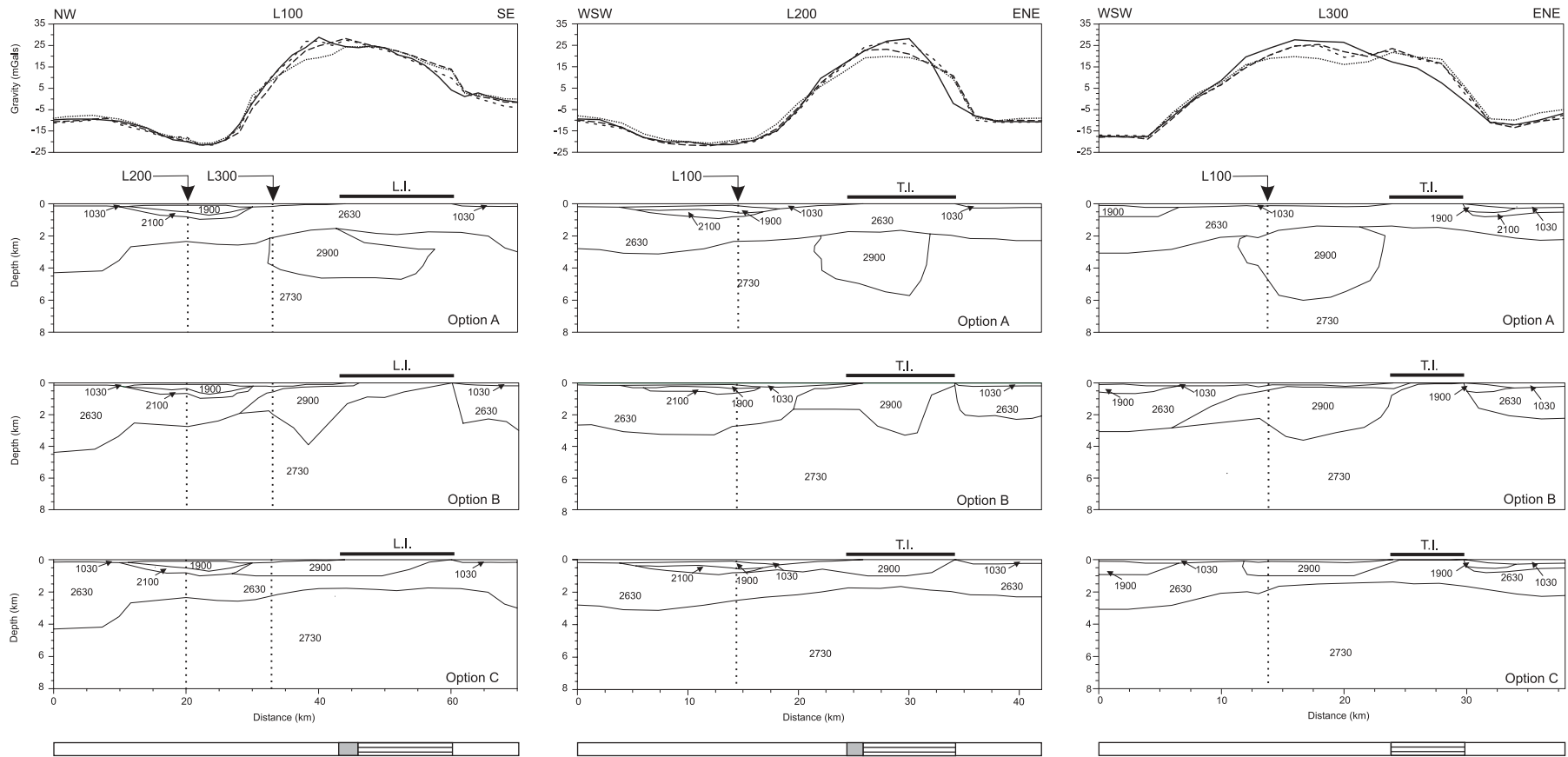
LEGEND

Geology

☐ Water
▨ Nanaimo Group
▤ Wrangellia
▨ Coast Belt

Gravity

— Observed
- - - Option A
··· Option B
········ Option C

gravity data support the interpretation of excess mass in the basement beneath the basin, most likely composed of the Karmutsen Formation, which represents one of the more dense lithologic components in Wrangellia (Table 2).

However, Lasqueti and Texada islands are primarily underlain by a Wrangellian stratigraphy that is presumed to persist to mid-crustal depths (England and Bustin 1998 and references therein). This stratigraphy, dominated by the Karmutsen Formation with lesser exposures of the Sicker Group, Quatsino Formation, and Island Intrusions, is higher density than the Nanaimo Group (Table 2), which underlies much of the offshore to the west and south of the islands. Therefore, seismic velocities beneath the islands should be higher than those observed in the adjacent offshore areas where basin-fill sediments occur, yet, this is not the case. Although seismic velocities are poorly constrained at depths < 1 km, at depths between 1 and 3 km velocities beneath the islands are indistinguishable from those of adjacent sediment-filled offshore areas. Thus, the interpreted geology is inconsistent with the seismic model in this region. To ascertain if gravity data can discriminate between these two interpretations, an alternative series of density models, consistent with the surface geology along the same three profiles, was developed (Fig. 6, Option B). This new series of models assumes that rocks with densities comparable to the Karmutsen Formation compose much of the upper 3–4 km beneath the anomalous region (2900 kg/m^3), whereas at greater depths rocks with an average Wrangellia density (2730 kg/m^3) prevail. The gravity responses of these models satisfy observed data just as well as those generated by the density models shown in Option A (Fig. 6), and we conclude gravity data alone cannot distinguish between the interpreted geology and seismic model in this region.

In the absence of additional constraints, compatibility of the surface geology and seismic model would require the Wrangellian stratigraphy exposed on the islands to be less than a kilometre thick (depth of poorly constrained velocity information), underlain by the Nanaimo Group to depths of ~3 km and at greater depths by a Wrangellian basement. This in turn implies that the Wrangellian stratigraphy exposed on the islands must be a tectonic flap emplaced along fault(s) with shallow crustal (≤1 km) offsets. However, there is no evidence for such faults, and gravity models (Option 3, Fig. 6) show that even if the entire upper 1 km beneath the anomalous region was composed of the Karmutsen Formation, the resulting gravity would significantly underestimate the peak anomaly along all three profiles. Consequently, we consider this option highly unlikely. Additional information on the upper 3–4 km of the crust beneath the islands is required to resolve the complex structure suggested by the geology and the seismic model.

Eastern limit of Wrangellia

The "local" scale gravity differences just discussed (anomalies 1 to 5, Fig. 5a) are superimposed on longer wavelength differences related to large-scale mass anomalies in the basement beneath the basin. To facilitate a more accurate analysis and interpretation of the latter, the sedimentary layers defined in the tomography and gravity models were used to compute and remove the gravity effect of the water and basin-fill. Densities for the four main layers of basin-fill (Ta-

ble 1, column b) and basement were kept consistent with earlier calculations. With the removal of gravity effects due to bathymetry and lower density sediments and sedimentary rocks, mass anomalies within the basement beneath the Strait of Georgia become clearly visible (Fig. 7).

For example, to the east of a "line" extending from Boundary Bay (SE) to Savory Island (NW), gravity values are generally lower than those observed to the west (dashed line, Fig. 7). Although both Wrangellia and the Coast Belt (which underlie Georgia Basin in this region, Fig. 1) contain rocks with a range of densities (Table 1), the proportion of mafic lithologies in Wrangellia is higher than that of the Coast Belt (Monger and Journeay 1994), and consequently, Wrangellian crust should have a higher average density. This being the case, areas underlain by Coast Belt rocks should have relatively lower measured gravity, and the transition from Wrangellia to Coast Belt, if relatively sharp, should appear as a negative gradient on the gravity map. Consequently, we infer that the pronounced west-to-east decrease in amplitude of the Bouguer anomaly observed across the study region from Boundary Bay to Savory Island marks the boundary between Wrangellia and the Coast Belt. The transition is also imaged, although more subtly, in the gravity difference data (Fig. 5a), where the observed gravity is compared with calculated values that assumed a constant density, Wrangellian-type lower crust.

Examination of several profiles across this boundary in the northern and central Strait of Georgia (including profiles A–A′, B–B′, and C–C′, Fig. 7) shows that the width of the negative gradient zone generally increases southward, although its amplitude remains relatively uniform. As the width of the anomaly is controlled, in large part, by the depth and dip of the density boundary, these observations suggest that either the Wrangellia – Coast Belt boundary shallows toward the southern Strait or Georgia, or the transition between the two basement units becomes broader, or possibly some combination of both these factors. Indeed, we note that to the south of Boundary Bay, the gravity gradient is diminished significantly and difficult to trace farther to the south with any confidence. Here, the Wrangellia – Coast Belt boundary may have been considerably disrupted by Eocene and younger deformation (Mustard and Rouse 1994; England and Bustin 1998; Journeay and Morrison 1999), or alternatively, it may be that a substantial thickness (i.e., mass) of high density Wrangellian lithologies does not persist south of Boundary Bay. Indeed, basement rocks of the Cascade Mountains are exposed on southern Lummi and Orcas islands ~25 km south of Boundary Bay.

The Wrangellia – Coast Belt transition that we have delineated parallels a strong gradient in magnetic anomaly data (Fig. 5b and 7). An investigation by Coles and Currie (1977) demonstrated that the mean surface magnetization on Vancouver Island is lower than that of the western Coast Belt, a fact supported by the magnetic susceptibility data presented in Table 2. These authors showed that, to depths of ~40 km, crust in the western Coast Belt has a significantly higher magnetization than crustal rocks beneath Vancouver Island, and they placed the boundary between these two disparate magnetic regions along the eastern margin of the Strait of Georgia very close to the location of our inferred Wrangellia – Coast Belt transition. In their interpre-

Fig. 7. Upper image shows the Bouguer anomaly resulting from the removal of the gravity effect of the water and sediment layers (see text for details). Broken line denotes the inferred Wrangellia – Coast Belt transition beneath the Strait of Georgia. The black star in central Strait of Georgia denotes the epicentre of the 1997 M 4.6 earthquake. Lower part of figure denotes gravity (solid) and magnetic (dashed) data along profiles A–A′, B–B′, and C–C′.
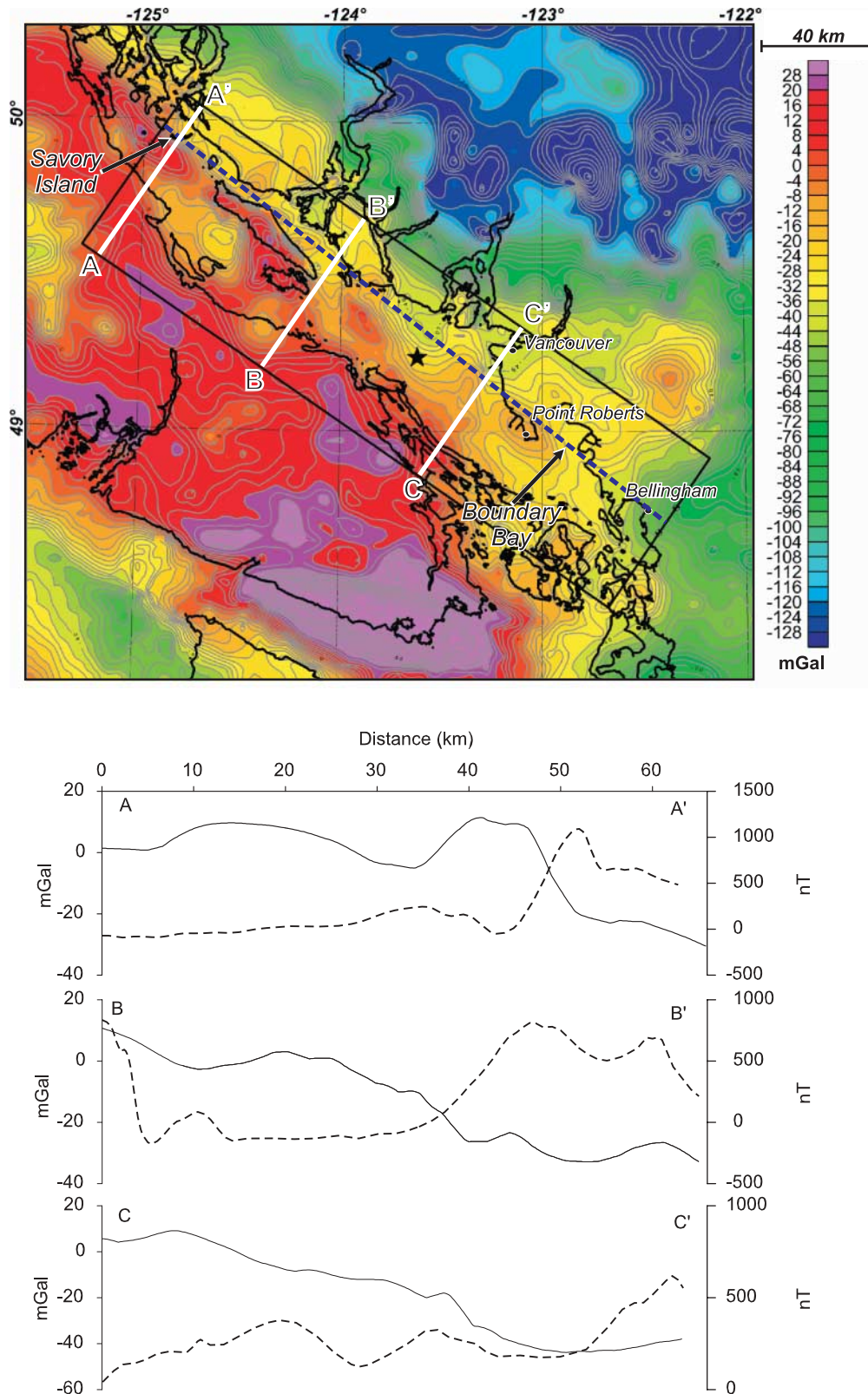
tation, these authors suggested that the magnetic crust at lower crustal depths in the Coast Belt is likely a secondary phenomenon, related to thermal reworking of crustal rocks above a dehydrated downgoing oceanic plate. Although not identical along strike, nonetheless, the general correspondence between our inferred Wrangellia – Coast Belt density transition and the eastern limit of the proposed thermally reworked crust is remarkable.

Our delineation of the Wrangellia – Coast Belt transition is consistent with information from some previous investigations. For example, Mulder (1995) used the differences between *P* and *S* arrival times of local earthquakes to estimate Poisson's ratio values of 0.253 ± 0.002 for the upper 30 km of Wrangellia on Vancouver Island, and 0.238 ± 0.004 for the upper 30 km of the western Coast Belt. On this basis, she concluded that the boundary between Wrangellia (Insular Superterrane) and the more felsic Coast Belt lay beneath the Strait of Georgia, although her data did not allow her to delineate its precise location or geometry. Clowes et al. (1997) modeled potential-field data across the Strait of Georgia using constraints provided by older 2-D seismic reflection and refraction profiles. They interpreted a northeast-dipping contact beneath the eastern Strait of Georgia as the boundary between Wrangellia and Coast Belt rocks and inferred that plutonic rocks of the Coast Belt extended throughout most of the crustal section. Most recently, Zelt et al. (2001) interpreted a lateral variation in sub-basin seismic velocities along a 2-D seismic profile in the Strait of Georgia as the transition from Wrangellia to Coast Belt basement rocks (Fig. 5*a*). The transition was traced to the base of their model at a depth of ~5 km. In an earlier study, Zelt et al. (1993) used a combination of travel-time inversion and forward modeling of seismic refraction data to compute the velocity structure beneath a 330 km transect extending from central Vancouver Island to Princeton on the mainland. In their interpretation, the Wrangellia – Coast Belt boundary is located beneath the eastern Strait of Georgia (close to our inferred boundary) at upper crustal depths, but at mid and lower crustal depths Wrangellia is thought to extend eastwards to the vicinity of the Harrison Fault (located ~100 km to the east of the study area).

In contrast, Friedman et al. (1990), Monger (1990, 1991), and Monger and Journeay (1994) consider the Bowen Island Group, exposed in the Howe Sound area, and the Harrison Lake Formation, exposed farther to the east, to be relics of a major volcanic-arc complex constructed either within or along the inboard margin of Wrangellia. Consequently, they place the eastern margin of Wrangellia and the Insular Superterrane well within the Coast Mountains.

The location of our inferred density transition between Wrangellia and the Coast Belt is essentially consistent with that delineated by Zelt et al. (2001) and Clowes et al. (1997), although our model does not constrain the geometry of the transition. Higher resolution seismic imaging of the middle and lower crust beneath the Strait of Georgia is required to determine if sub-basin lateral density differences persist at all crustal depths across this transition.

Comparison with the Puget Lowland area

Georgia Basin is just one in a series of sedimentary basins

located ~150 km inboard of the trench, between northern California and British Columbia (Dickinson 1976). The basins in British Columbia and northern Washington State, together with major faults, are superposed on the gravity map in Fig. 8. Presently, the direction of maximum crustal stress throughout the fore-arc region is margin parallel (Wang et al. 1995; Cassidy and Bostock 1996; Magee and Zoback 1992; Werner et al. 1991). Recent thrusting on a shallow northward-directed fault zone in Georgia Basin, as documented by Cassidy et al. (2000), is, not surprisingly, similar to that observed elsewhere in the fore arc: the 1995 M 5.0 (Dewberry and Crosson 1995) and 1997 M 4.9 (Weaver et al. 1999) events in the Puget Lowland were both associated with thrust faulting, possibly along the east-trending Seattle Fault that bounds the Seattle Basin along its southern margin. In fact, this observation, as well as other similarities in basin geometries, have led some workers to suggest that Georgia Basin has an origin similar to that of many other basins in the Puget Lowland (T. Brocher, personal communication, 2002; Mustard and Rouse 1994). Indeed, Rogers (1982) suggests that mineralogical phase changes within the subducting plate are responsible not only for the development of sedimentary basins within Cascadia, but also for those observed within the fore arcs of most shallow subducting plates.

Other workers have proposed distinct origins for basins within the Cascadia fore arc. For example, Crosson and Symons (2001) attribute development of five distinct basins, including the Seattle Basin in the northern Puget Lowland, to the uplift and subsequent erosion of the Crescent Terrane in the central Olympic Mountains. Their model does not explain the origin of basins farther to the north, or south, in the fore arc. Certainly, accretion of the Pacific Rim and Crescent terranes during the Eocene (Engebretson et al. 1985; Clowes et al. 1987), dextral strike-slip faulting in the western Cordillera during the Tertiary (Mustard and Rouse 1994), rapid uplift of the Coast Mountains during the Neogene (Parrish 1983), and the Miocene to recent uplift of the Olympic Mountains (Brandon et al. 1998) produced significant along-axis variations in the stress regime of the fore arc at earlier times in its evolution. However, to what extent these events triggered the development of individual basins, or simply produced second-order modifications of a single basin-forming mechanism is yet to be determined. Published geological reports and results from recent geophysical investigations spawned from the SHIPS experiment provide an opportunity to compare the crustal architecture along the fore arc from southern British Columbia to central Washington. The comparison points to profound differences in most aspects (i.e., age, geometry and depositional environments) of the sedimentary basins and the underlying fore-arc crust throughout this region.

For example, sedimentary fill in Georgia Basin ranges in age from Late Cretaceous to Recent, however, the oldest deposits in both the Seattle and Everett basins are Eocene in age (Johnson et al. 1994; Johnson et al. 1996). Although all three basins similarly comprise marine and nonmarine sedimentary strata, in the case of Georgia Basin, most of the Late Cretaceous Nanaimo Group strata were deposited in a marine environment, whereas Tertiary strata were deposited in a nonmarine environment. In Everett Basin the oldest (Eocene Chukanut Formation) and youngest (unnamed Miocene

Fig. 8. Gravity data (Bouguer onshore, free-air offshore) for northern Washington and southern British Columbia. Solid black lines denote the extent of the Seattle (SB), Everett (EB), and Georgia (GB) basins. Dashed lines denote faults discussed in text. CRBF, Coast Range Boundary Fault; DAF, Darrington Fault; DMF, Devil's Mountain Fault; HCF, Hood Canal Fault; LIF, Lummi Island Fault; LRF, Leech River Fault; OIF, Outer Islands Fault; SF, Seattle Fault; SJF, San Juan Fault; SWIF, South Whidby Island Fault.
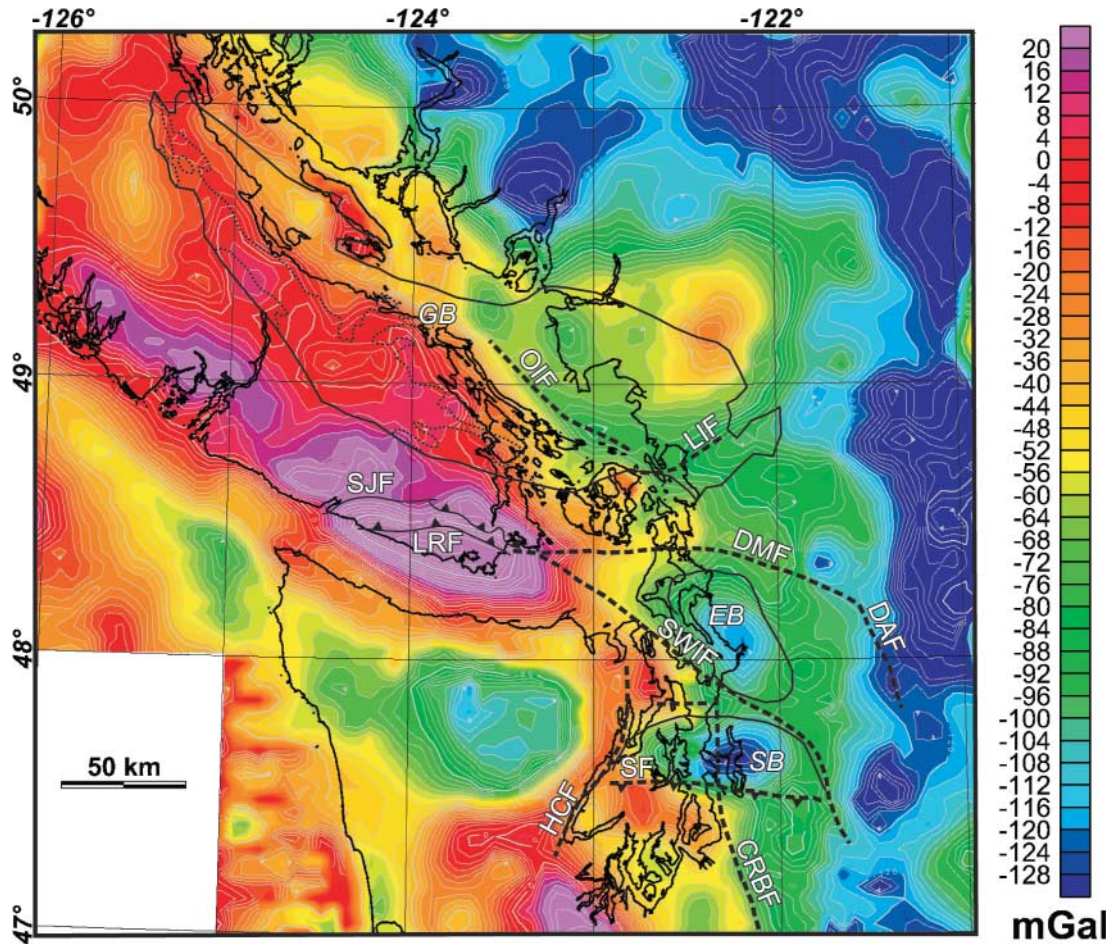
strata) sedimentary fill were deposited in a nonmarine environment, whereas intervening units were deposited in the shallow-marine environment (Johnson et al. 1996). In Seattle Basin, nonmarine strata are restricted to Miocene and younger age with all older units having been deposited in a marine environment (Johnson et al. 1994). Thus, there was differential uplift and migration of the paleoshoreline position along the axis of the fore arc throughout Tertiary times.

Georgia Basin is considerably larger than most of the basins in the Puget Lowland (Figs. 1, 8) with Late Cretaceous strata distributed over an area of 230 km × 90 km and Tertiary strata distributed over an area of 100 km × 50 km. The Seattle and Everett basins are 75 km × 30 km and 50 km × 30 km, respectively, (Brocher et al. 2001). Furthermore, as none of the original margins of the Late Cretaceous Georgia Basin are preserved, its actual extent during its initial phase of subsidence must have been significantly larger. Similarly, the areal extent of original Tertiary deposition within Georgia Basin is not well known, although provenance and sedimentological evidence presented in Mustard and Rouse (1994) suggest that it was probably not significantly more extensive than implied by the current outcrop patterns. Georgia and Everett basins are elongate in the northwesterly direction, deepening to the south and east. Seattle Basin is

elongate in the easterly direction, but deepening southward. The thickness of Tertiary and younger strata preserved in these basins decreases northward from ~9 km in Seattle Basin to just over 6 km in Everett Basin (Brocher et al. 2001) and to ~4 km in Georgia Basin (Zelt et al. 2001 and this study). Finally, Seattle and Everett basins are bounded on all sides by thrust or high angle faults that exhibit significant along-strike structural relief and that were active during sedimentation (Johnson et al. 1996). As noted earlier, none of the original boundaries of Georgia Basin are preserved, although today, the San Juan thrust system forms a fault boundary to Nanaimo Group strata along the southern boundary of the basin.

Gravity data highlight many of these differences in the fore arc. In general, the faults that bound the Seattle and Everett basins correlate with prominent linear and curvilinear zones of steep gravity gradient and the basins themselves with well-defined gravity lows, clearly isolated from adjacent anomalies (Fig. 8). In contrast, strong gravity gradients are absent around the eroded edges of Georgia Basin, and although anomaly values are lowest over the thicker and younger sedimentary accumulations within this basin, the amplitude of the gravity minimum is significantly less than that observed over the Seattle Basin despite comparable sedimentary thicknesses. In part, this may be attributed to the greater thick-

ness of older (and denser) sedimentary rocks within Georgia Basin, as well as to the smaller contrast between these units and the underlying basement (density contrast in Georgia Basin is -100 kg/m^3, Table 2; density contrast in Seattle Basin is estimated at -310 kg/m^3, Brocher et al. 2001).

With all of these new details on fore arc architecture, crustal composition, and the timing and extent of sedimentation and deformation events emerging, the next step has to be the development of kinematic models that allow the roles and effects of individual tectonic events to be quantitatively established. Only by doing so can we hope to answer the question of one, or many triggers for fore arc sedimentation within Cascadia.

Conclusions

(1) Forward modelling of the tomographically derived velocity model for Georgia Basin (Zelt et al. 2001) indicates that it is generally consistent with the observed gravity field. Some discrepancies are attributed to resolution of the tomography model.

(2) Measured densities from surface rocks provide better results than do values estimated through conversion of seismic velocities using the Gardner et al. (1974) relationship. This contrasts with results from basins in the Puget Lowland, where Gardner et al.'s relation provided satisfactory results; however, the reason for the difference has not been fully investigated.

(3) Analysis of gravity residuals delineates four areas in offshore Georgia Basin with significant accumulations of unconsolidated sediments. Improved geophysical imaging and direct sampling of these regions is needed to assess their aggregate potential and susceptibility to failure during seismic events.

(4) The study highlights an incompatibility between geological interpretations and the upper-crustal velocity structure beneath Texada and Lasqueti islands, central Strait of Georgia. However, gravity data alone cannot discriminate between the geologic and seismic models in this area.

(5) A distinct gradient trending along the eastern side of the Strait of Georgia is interpreted as marking the upper crustal transition of Wrangellia to the Coast Belt. The interpretation is consistent with independent seismic and magnetic data.

(6) Comparison of Georgia Basin with the Seattle and Everett basins to the south shows distinct differences in gravity signature, most notably the reduced amplitude of the gravity minimum and the lack of steep gradients bounding Georgia Basin. Major differences in the geometry, age, and nature of the sedimentary fill are also recognized. Collectively, the differences imply significant along-axis variations in fore arc deposition and deformation throughout Mesozoic and Tertiary times. In contrast, similar focal mechanisms for recent earthquakes along generally east-trending faults, and a common margin-parallel stress regime suggest that a single mechanism is controlling present-day basin tectonics and deformation in these regions.

References

Barrie, J.V., and Conway, K.W. 2000. A preliminary interpretation of surficial marine geology of central and northern Strait of Georgia, British Columbia. *In* Current research. Geological Survey of Canada, Paper 2000-A, 7 pages.

Brandon, M.T., Roden-Tice, M.K., and Garver, J.I. 1998. Late Cenozoic exhumation of the Cascadia accretionary wedge in the Olympic Mountains, northwest Washington State. Geological Society of America, Bulletin, **110**: 985–1009.

Brocher, T.M., Parsons, T., Blakely, R.E., Christensen, N.I., Fisher, M.A., Wells, R., and the SHIPS Working Group 2001. Upper crustal structure in Puget Lowland, Washington: Results from the 1998 seismic hazards investigation in Puget Sound. Journal of Geophysical Research, **106:** 13541–13564.

Cassidy, J.F., and Bostock, M.G. 1996. Shear-wave splitting above the subducting Juan de Fuca plate. Geophysical Research Letters, **23**: 941–944.

Cassidy, J.F., Rogers, G.C., and Waldhauser, F. 2000. Characterization of active faulting beneath the Strait of Georgia, British Columbia. Bulletin of the Seismological Society of America, **90**: 1188–1199.

Clague, J.J. 1977. Quadra Sand: a study of the Late Pleistocene geology and geomorphic history of coastal southwest British Columbia. Geological Survey of Canada, Paper 1977-17.

Clague, J.J., Luternauer, J.L., and Hebda, R.J. 1983. Sedimentary environments and postglacial history of the Fraser Delta and lower Fraser Valley, British Columbia. Canadian Journal of Earth Sciences, **20**: 1314–1326.

Clowes, R.M., Brandon, M.T., Green, A.G., Yorath, C.J., Sutherland-Brown, A., Kanasewich, E.R., and Spencer, C. 1987. LITHOPROBE—southern Vancouver Island: Cenozoic subduction complex imaged by deep seismic reflection. Canadian Journal of Earth Sciences, **24**: 31–51.

Clowes, R.M., Baird, D.J., and Dehler, S.A. 1997. Crustal structure of the Cascadia subduction zone, southwestern British Columbia, from potential field and seismic studies. Canadian Journal of Earth Sciences, **34**: 317–335.

Coles, R.L., and Currie, R.G. 1977. Magnetic anomalies and rock magnetizations in the southern Coast Mountains, British Columbia: possible relation to subduction. Canadian Journal of Earth Sciences, **14**: 1753–1770.

Crosson, R.S., and Symons, N.P. 2001. Flexural origin of the Puget Basins: Implications for the Seattle Fault and Puget Basin Tectonics. EOS, Transactions of the American Geophysical Union, **82**: F856.

Dallimore, S.R., Edwardson, K.A., Hunter, J.A., Clague, J.J., and Lutenauer, J.L. 1995. Composite geotechnical logs for two deep

boreholes in the Fraser River Delta, British Columbia. Geological Survey of Canada, Open File Report 3018.

Dehler, S.A., and Clowes, R.M. 1992. Integrated geophysical modelling of terranes and other structural features along the western Canadian margin. Canadian Journal of Earth Sciences, **29**: 1492–1508.

Dewberry, S.R., and Crosson, R.S. 1995. Source scaling and moment estimation for the Pacific Northwest Seismograph Network using S-coda. Bulletin Seismological Society of America, **85**: 1309–1326.

Dickinson, W.R. 1976. Sedimentary basins developed during evolution of Mesozoic-Cenozoic arc-trench system in western North America. Canadian Journal of Earth Sciences, **13**: 1268–1287.

Engebretson, D.C., Cox, A., and Gordon, R.G. 1985. Relative motions between oceanic and continental plates in the Pacific Basin. Geological Society of America, Special Paper 206.

England, T.D.J., and Bustin, R.M. 1998. Architecture of the Georgia Basin southwestern British Columbia. Bulletin of Canadian Petroleum Geology, **46**: 288–320.

Fisher, M.A., Brocher, T.M., Hyndman, R.D., Trehu, A.M., Weaver, C.S., Creager, K.C., Crossan, R.S., Parsons, T., Cooper, A.K., Mosher, D., Spence, G., Zelt, B.C., Hammer, P.T.C., ten Brink, U., Pratt, T.L., Miller, K.C., Childs, J.R., Cochrane, G.R., Chopra, S., and Walia, R. 1999. Seismic survey probes urban earthquake hazards in Pacific Northwest. EOS, Transactions of the American Geophysical Union, **80**: 13–17.

Friedman, R.M., Monger, J.W.H., and Tipper, H.W. 1990. Age of the Bower Island Group, southwestern Coast Mountains, British Columbia. Canadian Journal of Earth Sciences, **27**, 1456–1461.

Gardner, G.H.F., Gardner, L.W., and Gregory, A.R. 1974. Formation velocity and density; the diagnostic basics for stratigraphic traps. Geophysics, **39**: 770–780.

Hamilton, T.S. 1991. Seismic stratigraphy of unconsolidated sediments in the central Strait of Georgia: Hornby Island to Roberts Bank. Geological Survey of Canada, Open File 2530 (9 sheets).

Hora, Z.D. 1998. Aggregate resources of the Greater Vancouver and Lower Mainland market, B.C., Canada; problems and future outlook. *In* Aggregate resources; a global perspective. *Edited by* P.T. Bobrowsky. A.A. Balkema, Rotterdam, pp. 397–408.

Hunter, J.A.M., Burns, R.A., Good, R.L., and Pelletier, C.F.A. 1998. Compilation of shear wave velocities and borehole geophysics logs in unconsolidated sediments of the Fraser River Delta, British Columbia. Geological Survey of Canada, Open File D3622.

Johnson, S.Y. 1984. Stratigraphy, age and paleogeography of the Eocene Chukanut formation, northwest Washington. Canadian Journal of Earth Sciences, **21**: 92–106.

Johnson, S.Y., Potter, C.J., and Armentrout, J.M. 1994. Origin and evolution of the Seattle Fault and Seattle Basin, Washington. Geology, **22**: 71–74.

Johnson, S.Y., Potter, C.J., Armentrout, J.M., Miller, J.J., Finn, C., and Weaver, C. 1996. The southern Whidby Island fault: An active structure in the Puget Lowland, Washington. Geological Society of America, Bulletin, **108**: 334–354.

Journeay, J.M., and Morrison, J. 1999. Field investigation of Cenozoic structures in the northern Cascadia forearc, southwestern British Columbia, Canada. *In* Current research. Geological Survey of Canada, 1999-A/B, 239–250.

Magee, M.E., and Zoback, M.L. 1992. Well breakout analysis for determining tectonic stress orientations in Washington State. U.S. Geological Survey, Open File Report 92-715.

Mathews, W.H., and Shepard, F.P. 1962. Sedimentation of the Fraser River delta, British Columbia. American Association of Petroleum Geologists, Bulletin, **46**: 1416–1438.

Monger, J.W.H. 1990. Georgia Basin: Regional setting and adjacent Coast Mountains geology, British Columbia. *In* Current research. Geological Survey of Canada, Paper 90-1F, pp. 95–107.

Monger, J.W.H. 1991. Georgia Basin Project: Structural evolution of parts of southern Insular and southwestern Coast Belts. *In* Current research. Geological Survey of Canada, Paper 91-1A, pp. 219–229.

Monger, J.W.H., and Journeay, J.M. 1994. Basement geology and tectonic evolution in the Vancouver region. *In* Geology and geological hazards of the Vancouver region, southwestern British Columbia. *Edited by* J.W.H. Monger. Geological Survey of Canada, Bulletin 481, pp. 3–25.

Mosher, D.C., and Hamilton, T.S. 1998. Morphology, structure and stratigraphy of the offshore Fraser Delta and adjacent Strait of Georgia. *In* Geology and natural hazards of the Fraser River Delta, British Columbia. *Edited by* J.J. Clague, J.L. Lautenauer and D.C. Mosher. Geological Survey of Canada, Bulletin 525, pp. 147–160.

Mulder, T.L. 1995. Small earthquakes in southwestern British Columbia (1975–1991), M.Sc. thesis, University of Victoria, Victoria, B.C.

Mustard, P.S. 1994. The Upper Cretaceous Nanaimo Group, Georgia Basin. *In* Geology and geological hazards of the Vancouver region, southwestern British Columbia. *Edited by* J.W.H. Monger. Geological Survey of Canada, Bulletin 481, pp. 27–95.

Mustard P.S., and Rouse, G.E. 1994. Stratigraphy and evolution of Tertiary Georgia Basin and subjacent Upper Cretaceous sedimentary rocks, southwestern British Columbia and northwestern Washington State. *In* Geology and geological hazards of the Vancouver region, southwestern British Columbia. *Edited by* J.W.H. Monger. Geological Survey of Canada, Bulletin 481, pp. 97–169.

Parker, R.L. 1972. The rapid calculation of potential anomalies. Geophysical Journal of the Royal Astronomical Society, **31**: 447–455.

Parrish, R.R. 1983. Cenozoic thermal evolution and tectonics of the Coast Mountains of British Columbia: 1. Fission track dating, apparent uplift rates and patterns of uplift. Tectonics, **2**: 601–631.

Riddihough, R.P. 1979. Gravity and structure of an active margin— British Columbia and Washington, Canadian Journal of Earth Sciences, **14**: 384–396.

Rogers, G.C. 1982. The role of phase changes in the development of forearc basins. EOS, Transactions of the American Geophysical Union, **63**: 1113.

Smith, W.H.F., and Wessel, P. 1990. Gridding with continuous curvature splines in tension. Geophysics, **55**: 293–305.

Wang, K., Mulder, T., Rogers, G.C., and Hyndman, R.D. 1995. Case for very low coupling on the Cascadia subduction fault. Journal of Geophysical Research, **100**: 12,907–12,918.

Weaver, C.S., Meagher, K.L., Qamar, A., Blakely, R.J., and Wells, R.E. 1999. The June 23, 1997 Bainsbridge Island, Washington, Earthquake: evidence that the Seattle Fault is seismically active. Seismmological Research Letters, **70**: 219 (abstract).

Werner, K.S., Graven, E.P., Berkman, T.A., and Parker, M.J. 1991. Direction of maximum horizontal compression in western Oregon determined from borehole breakouts. Tectonics, **10**: 948–958.

Zelt, B.C., Ellis, R.M., and Clowes, R.M. 1993. Crustal velocity structure in the eastern Insular and southernmost Coast Belts, Canadian Cordillera. Canadian Journal of Earth Sciences, **30**: 1014–1027.

Zelt, B.C, Ellis, R.M., Clowes, R.M., and Hole, J.A. 1996. Inversion of three-dimensional wide-angle seismic data from southwestern Canadian Cordillera. Journal of Geophysical Research, **101**: 8503–8529.

Zelt, B.C., Ellis, R.M., Zelt, C.A., Hyndman, R.D., Lowe, C., Spence, G.D., and Fisher, M.A. 2001. Three-dimensional crustal velocity structure beneath the Strait of Georgia, British Columbia. Geophysical Journal International, **144**: 695–712.